



Clinical value of contrast-enhanced ultrasound quantitative analysis for differentiating thyroid lesions in Hashimoto's thyroiditis patients

Wanting Yang¹, Jiehong Zhou¹, Can Yue¹, Yushuang He¹, Jianyong Lei², Yong Chen¹, Buyun Ma^{1^}

¹Department of Medical Ultrasound, West China Hospital, Sichuan University, Chengdu, China; ²Division of Thyroid Surgery, Department of General Surgery, West China Hospital, Sichuan University, Chengdu, China

Contributions: (I) Conception and design: B Ma, J Lei, W Yang, J Zhou; (II) Administrative support: B Ma, J Lei; (III) Provision of study materials or patients: W Yang, J Zhou, Y He, C Yue; (IV) Collection and assembly of data: W Yang, J Zhou, Y He, C Yue, Y Chen; (V) Data analysis and interpretation: W Yang, J Zhou, Y Chen; (VI) Manuscript writing: All authors; (VII) Final approval of manuscript: All authors.

Correspondence to: Buyun Ma, MD. Department of Medical Ultrasound, West China Hospital, Sichuan University, 37 Guoxue Lane, Chengdu 610041, China. Email: ws_mby@126.com.

Background: The role of quantitative contrast-enhanced ultrasound (CEUS) in the evaluation of thyroid nodules with Hashimoto's thyroiditis (HT) has received little attention.

Methods: This was a retrospective cohort study. We consecutively enrolled 242 patients (49 males, 193 females, average age 52 years) with a combined total of 248 thyroid nodules coexisting with HT who underwent biopsy/resection-proven pathology from December 2016 to June 2021. All patients underwent preoperative ultrasound (US) and CEUS examinations performed by 2 radiologists independently. Quantitative analysis of CEUS using time-intensity curves (TIC) was measured by an expert radiologist from the thyroid intra-nodule and the surrounding parenchyma and their ratios. Receiver operating characteristic (ROC) analysis was performed to evaluate their diagnostic performance.

Results: The patients were divided into the nodular HT (NHT) group (n=42), the papillary thyroid carcinoma (PTC) group (n=154), and the primary thyroid lymphoma (PTL) group (n=52) according to their pathological results. TIC parameters revealed that PTC and PTL showed faster time to peak (TTP) (P=0.044, P=0.049), lower peak intensity (PI) (both P<0.001), and smaller areas under the curve (both P<0.001) than those of NHT. The intra nodule of PTL showed an obviously slower perfusion (ratio =0.90, P<0.001) and lower PI (ratio =0.84, P<0.001) compared with the thyroid parenchyma. TIC improved performance in distinguishing PTL from NHT [area under the curve (AUC): 0.947, 95% confidence interval (CI): 0.903–0.991], but inferior performance in differentiating PTC and NHT (AUC: 0.838, 95% CI: 0.759–0.917).

Conclusions: CEUS quantitative analysis could be valuable in differentiating thyroid malignancies in patients with HT.

Keywords: Thyroid nodules; ultrasonography; contrast media; Hashimoto's thyroiditis (HT)

Submitted May 01, 2023. Accepted for publication Nov 09, 2023. Published online Nov 27, 2023.

doi: 10.21037/qims-23-601

View this article at: <https://dx.doi.org/10.21037/qims-23-601>

[^] ORCID: 0000-0003-1201-3354.

Introduction

Among endocrine malignancies, the incidence of thyroid cancer has increased substantially over the past 50 years (1). It is the 9th most common disease globally, with 586,000 cases reported in 2020 (2). A link between inflammation and cancer is well-known (3). Hashimoto's thyroiditis (HT) is now considered the most prevalent autoimmune disease, as well as the leading cause of hypothyroidism (4). In fact, in HT, the gland microenvironment is characterized by the presence of infiltrating lymphocytes and other immune competent cells (5). It has been hypothesized that chronic inflammatory stimulus and immune processes may be linked to tumorigenesis among certain tissues, and can lead to neoplastic transformation through an oncogene signaling pathway that is induced by the expression of inflammation-related genes (3). Although still inconsistent, epidemiological and histological data have indicated that HT has a strong association with papillary thyroid carcinoma (PTC) and primary thyroid lymphoma (PTL) (6-8). Unlike other types of thyroid cancer, thyroid lymphoma arises from lymphocytes, most commonly B lymphocytes (9). Patients with HT are at greater risk for developing PTL, with a relative risk of 40- to 80-fold compared to those without thyroiditis (10). Epidemiologic studies have reported that HT is found in 20–50% of PTC samples and it is linked itself to a higher risk of PTC (11).

Ultrasound (US) is used as the basis for several thyroid nodule risk stratification systems (12). Unfortunately, none of the existing recommendations specifically address how to deal with the nodules with a background of diffuse HT, whereby patients have both a sonographically abnormal gland and an increased risk of malignancy. Chronic inflammation causes damage to surrounding tissues and blood vessels, resulting in US characteristics of heterogeneous hypo-echoic thyroid parenchyma, micronodulation, and hypervascularity (13). HT may form discrete nodules within a diffusely altered parenchyma known as nodular HT (NHT) (14). NHT largely underscores the difficulty in distinguishing from malignant nodules due to its more hypoechoic and heterogeneous appearance with irregular margins, leading to an unnecessary biopsy rate (15,16).

Contrast-enhanced ultrasound (CEUS) is an efficient technique to evaluate the vascularity distribution and hemodynamics of tumors compared to tumor-surrounding tissues (17). CEUS focuses on displaying the microvasculature of tissues, and the contrast agent used

is a pure blood-pool, negating some of the limitations of Doppler US in the assessment of the microvascular flow pattern in tumorous lesions (18). Doppler US helps to characterize blood flow, with limitations of attenuation, low sensitivity for very slow blood flow, and angle dependency (19). The European Federation of Societies for Ultrasound in Medicine and Biology (EFSUMB) guidelines suggested that CEUS allowed reliable diagnostics (20). The pooled sensitivity, specificity, and accuracy of CEUS for diagnosing malignant thyroid nodules have been reported to be 76.9–88.2%, 84.8–95.1%, and 82.6–90.4%, respectively (21). However, CEUS features in thyroid nodules lack consensus reporting standards, leading to bias between results from different observers. Thus, the introduction of a time-intensity curve (TIC) to evaluate and characterize the information of the microvascular density of the thyroid nodules is highly important. Most studies focusing on the diagnosis of thyroid lesions using a TIC have concentrated mainly on normal parenchyma (22-24).

To further extend those prior reports, our study aimed to retrospectively evaluate the diagnostic performance of CEUS based on quantitative enhancement analysis in the differentiation of thyroid nodules accompanied with HT. We present this article in accordance with the STARD reporting checklist (available at <https://qims.amegroups.com/article/view/10.21037/qims-23-601/rc>).

Methods

Patients

The study was conducted in accordance with the Declaration of Helsinki (as revised in 2013). This retrospective cohort study was approved by the institutional review board of the West China Hospital, Sichuan University, Chengdu, China (No. 20230927). The committee waived the requirement for individual consent for this retrospective analysis. The US images and CEUS videos of patients who underwent thyroid biopsy/surgery were consecutively collected in West China Hospital from December 2016 to June 2021, with the following inclusion criteria (*Figure 1*): (I) ≥ 18 years old; (II) US and CEUS exams within 3 months before percutaneous biopsy or surgical resection; (III) thyroid parenchyma was clinically confirmed as HT; and (IV) thyroid nodules had reliable pathological diagnosis. Patients were excluded if they (I) had a history of ablation; and (II) had nodules with diameter < 1 cm.

The clinical diagnosis of HT is currently established

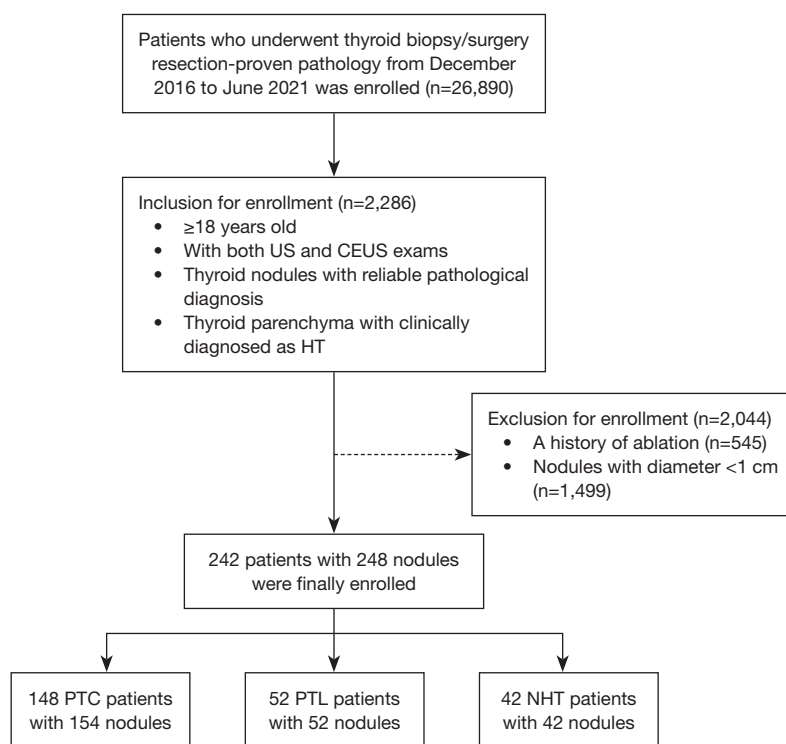


Figure 1 Flow diagram of our study population. US, ultrasound; CEUS, contrast-enhanced ultrasound; HT, Hashimoto's thyroiditis; PTC, papillary thyroid carcinoma; PTL, primary thyroid lymphoma; NHT, nodular Hashimoto's thyroiditis.

by serum antibodies against thyroid antigens (mainly thyroperoxidase ≥ 34 IU/mL or thyroglobulin ≥ 115 IU/mL). The pathological features suggest that HT may be present. All of our patients were diagnosed with HT by serum antibodies against thyroid antigens.

US and CEUS examination

The gray-scale US and CEUS examinations were performed using a US system (iU22, Phillips Healthcare, Bothell, WA, USA) with a 5–12 MHz linear probe for gray-scale US and a 3–9 MHz linear probe for CEUS. CEUS was performed using reverse pulse imaging technique with a real-time, low-mechanical index (MI = 0.06). A contrast medium SonoVue (1.0–2.0 mL; Bracco, Milan, Italy) bolus was injected intravenously, followed by injection of 0.9% sodium chloride solution (5 mL). The image focus was placed below the region of interest (ROI) and a dual screen format was used for all the CEUS examinations showing a gray-scale image alongside the contrast-specific image. The image was dynamically observed after the bolus, and the timer on the US system was initiated simultaneously.

The CEUS dynamic videos were recorded continuously for at least 3 minutes for further analysis. The set of CEUS imaging was stored on the hard drive of the US system and copied to portable hard drive for later evaluation.

US and CEUS image analysis

The images were reviewed by two radiologists (C.Y. and Y.H. with at least 5 years of experience in US and at least 2 years of experience in CEUS of the thyroid gland and neck area) who were blinded to clinical information and pathological results and recorded their judgments independently. Interobserver agreement on the baseline qualitative US and CEUS imaging features was evaluated by the kappa value. If no consensus was reached, discrepancies were resolved by the judgement of a third reviewer (B.M., with 20 years' experience in head and neck US and 10 years in CEUS).

The conventional US (gray-scale US and color Doppler US) features of each nodule were evaluated as follows: size on US (maximum diameter); inner echogenicity (very hypo-, hypo-, or hyper-/iso-echoic); shape (taller than

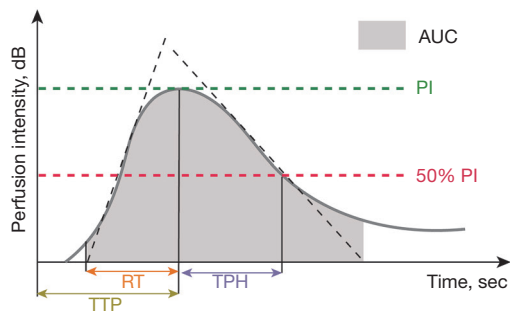


Figure 2 The perfusion parameters obtained from the time intensity curve analysis of the Contrast-enhanced ultrasound examination. AUC, area under the curve; PI, peak intensity; RT, rise time; TTP, time to peak; TPH, time from peak to one-half.

wide or wider than tall); margin (smooth or ill-defined, lobulated, or irregular, extrathyroidal extension); posterior acoustic enhancement (normal, attenuation, enhancement); calcification (none, micro, or macro); Adler grade [Grade 0: no blood flow in the lesion; Grade 1: 1–2 pixels contained blood flow (usually <1 mm in diameter) was observed in the lesion; Grade 2: 3–4 pixels or a main vessel were visualized in the lesion; Grade 3: ≥ 5 pixels or ≥ 2 main vessels were visualized inside the lesion] (25). Nodules were classified according to the American College of Radiology (ACR) Thyroid Imaging Reporting and Data System (TI-RADS) lexicon (26) and User's Guide (27).

The CEUS imaging features were assessed including the enhancement pattern (homogeneous or heterogeneous), the degree (hypo-, iso-, or hyper-enhancement), and the direction (centripetal/centrifugal or scattered perfusion). Homogeneous lesions were defined as those in which the entire lesion showed uniform and diffuse enhancement at the time of peak intensity (PI), regardless of the extent of enhancement. Heterogeneous lesions, on the other hand, were defined as enhanced lesions that contain partial enhancement. Centripetal/centrifugal enhancement was characterized by microbubbles expanding from either the margins of the nodule towards the center, or from the center towards the margins. The nodules showed hypo-/iso-/hyper-enhancement, which was detected as decreased/the same/increased internal echogenicity compared to the surrounding thyroid tissue.

The TIC analysis of nodules was performed with Q-LAB software (Philips Healthcare, USA) (Figure 2). A radiologist (B.M.) manually defined the ROI that was placed on the thyroid nodules on each image. A second ROI was drawn in the adjacent thyroid parenchyma as an internal reference. It

was ensured that both ROIs were located at the same level, the same depth, and were of similar size.

Perfusion parameters: (I) PI (dB), defined as the maximal signal intensity measured in the selected ROI; (II) time to peak (TTP, seconds), defined as the time from the starting point to the PI of the curve; (III) rise time (RT, seconds), defined as the time from the instant where the maximum slope tangent intersects the x-axis to the peak. Clearance parameters: time from peak to one-half (TPH, seconds), defined as the time from the peak point to the PI drop to 50% of the curve. Comprehensive parameters: (I) mean transit time (MTT, seconds), defined as the time from the starting point to the PI drop to 50% of the curve; and (II) area under the curve (AUC), defined as the area under the whole-time intensity curve.

Pathologic analysis

The histological results were the reference diagnostic standard. A tissue sample of the lesion was obtained by surgical resection or biopsy. The pathological diagnoses of nodules were confirmed according to the World Health Organization (WHO) classification of tumors (28).

HT pathological features are associated with lymphoplasmacytic infiltration with germinative center formation, oxyphilic cell metaplasia (Hürthle), atrophy, and fibrosis of thyroid follicles were classified as HT (5).

Statistical analysis

Categorical variables were summarized using frequencies and percentages, whereas continuous variables were summarized using the median and interquartile range and mean and standard deviation. The Mann-Whitney *U* test was used for continuous variables, and the χ^2 or Fisher exact test was used for categorical variables. Logistic regression analysis was used for univariate analysis of all parameters. Then, the absolute and relative parameters that were statistically related to malignant nodules at a level of significance of $P < 0.05$ (two-sided) were included in a multivariate logistic regression analysis model to identify independent risk factors for malignancies. Multivariate logistic regression analysis was used to develop AUCs based on the optimal features for diagnosing. The AUCs with 95% confidence intervals (CIs) were compared using the DeLong test. Interobserver agreement in analyzing the imaging features of thyroid nodules was evaluated with Cohen's kappa coefficient. A κ value < 0.2 indicated

Table 1 Clinical characteristics of 242 study patients with 248 thyroid nodules combined with Hashimoto's thyroiditis

Parameters	PTL	PTC	NHT	P	
				PTL vs. NHT	PTC vs. NHT
No. of patients	52	148	42		
No. of nodules	52	154	42		
Sex [†]				0.005*	0.035*
Female	37 (71.2)	117 (79.1)	39 (92.9)		
Male	15 (28.8)	31 (20.9)	3 (7.1)		
Age [‡] (year)	58.7±9.3	49.5±17.6	46.6±12.4	<0.001*	0.005*
Size [‡] (mm)	49.9±18.9	17.2±6.9	18.2±7.6	<0.001*	0.501

[†], data are numbers of patients, with percentages in parentheses. [‡], data are means ± SDs. *, P<0.05 was considered statistically significant. PTL, primary thyroid lymphoma; PTC, papillary thyroid carcinoma; NHT, nodular Hashimoto's thyroiditis; SD, standard deviation.

poor agreement; 0.2–0.4 indicated fair agreement; 0.41–0.6 indicated moderate agreement; 0.61–0.8 indicated good agreement; and 0.81–1.00 indicates almost perfect agreement. Data were analyzed with SPSS 26.0 (IBM Corp., Armonk, NY, USA) and MedCalc, version 15.0 (MedCalc Software, Ostend, Belgium). A P value <0.05 was considered indicative of a statistically significant difference.

Results

Patients and thyroid nodules characteristics

On the basis of the selection criteria, 242 patients with 248 thyroid nodules were enrolled, which included 42 NHT patients (3 male and 39 female; average age 46.6±12.4 years), 52 PTL patients (15 male and 37 female; average age 58.7±9.3 years), and 148 PTC patients (31 male and 117 female; average age 49.5±17.6 years). Among these nodules, the mean size of 42 NHT nodules was 18.2±7.6 mm, 52 PTL nodules was 49.9±18.9 mm, and 154 PTC nodules was 17.2±6.9 mm. The patients with PTL were significantly older (P<0.001) and their nodules had larger size (P<0.001) than those with NHT. Clinical characteristics of patients including age, sex, nodule size, and tumor histopathologic results are displayed in *Table 1*.

Comparison of qualitative analysis

Interobserver agreement in two readers (C.Y. and Y.H.) in US and CEUS of the thyroid had excellent interobserver agreement with κ value of 0.81. In terms of qualitative analysis for the gray-scale US features (*Table 2*), PTC

appeared more frequently as taller than wide shape (61.7% vs. 16.7%, P<0.001), extrathyroidal extension margin (76.6% vs. 16.7%, P=0.009), micro-calcification (66.2% vs. 4.8%, P<0.001), and posterior echo attenuation (20.8% vs. 0.0%, P<0.001) than NHT on gray-scale US. PTL tended to have posterior echo enhancement (46.2% vs. 16.7%, P<0.001) and intra-nodular visualized vascularity (Adler grade 0: 5.8% vs. 23.8%, P<0.001) more than NHT. Compared with NHT, the CEUS parameters of PTL and PTC were more likely to be centripetal/fugal, heterogeneous and hypo-enhancement (all P<0.001) (*Table 3*).

Comparison of quantitative analysis

As shown in *Table 4*, perfusion parameters: in malignant lesions (PTC and PTL), the PI was significantly lower (P<0.001, P<0.001) and TTP (P=0.044, P=0.049) was faster than those of NHT. RT in PTC nodule was significantly faster (P=0.029) than in NHT. The ratios of lesion and background in PI, RT, and TTP between PTL and NHT were significantly different. PTL showed that the PI (ratio =0.84 vs. 0.97, P<0.001) of intra-lesions were much lower than their backgrounds, or RT (ratio =0.89 vs. 0.97, P<0.001) and TTP (ratio =0.90 vs. 1.00, P<0.001) of intra-lesions presented much faster.

Clearance parameters: compared with NHT, TPH in PTL was significantly longer (P<0.001).

Comprehensive parameters: AUC in PTL and PTC were significantly smaller than in NHT (P<0.001, P<0.001).

In this study, NHT and PTC nodules were divided into two groups (10–<20 and ≥20 mm), and PTL nodules were divided into two groups (10–<50 and ≥50 mm), according

Table 2 Comparison of US qualitative parameters in thyroid nodules combined with Hashimoto's thyroiditis

US parameters	PTL (n=52), No. (%)	PTC (n=154), No. (%)	NHT (n=42), No. (%)	P	
				PTL vs. NHT	PTC vs. NHT
Echogenicity				0.184	0.202
Very hypoechoic	4 (7.7)	0	0		
Hypoechoic	47 (90.4)	142 (92.2)	41 (97.6)		
Hyper/iso-echoic	1 (1.9)	12 (7.8)	1 (2.4)		
Shape				0.866	<0.001*
Wider than tall	44 (84.6)	59 (38.3)	35 (83.3)		
Taller than wide	8 (15.4)	95 (61.7)	7 (16.7)		
Margin				0.042*	0.009*
Smooth or ill-defined	7 (13.5)	3 (1.9)	9 (21.4)		
Lobulated or irregular	24 (46.2)	33 (21.4)	26 (61.9)		
Extrathyroidal extension	21 (40.4)	118 (76.6)	7 (16.7)		
Calcification				0.280	<0.001*
None	45 (86.5)	31 (20.1)	40 (95.2)		
Micro	5 (9.6)	102 (66.2)	2 (4.8)		
Macro	2 (3.8)	21 (13.6)	0		
Posterior echo				<0.001*	<0.001*
Normal	28 (53.8)	121 (78.6)	35 (83.3)		
Attenuation	0	32 (20.8)	0		
Enhancement	24 (46.2)	1 (0.6)	7 (16.7)		
Adler				<0.001*	0.122
Grade 0	3 (5.8)	35 (22.7)	10 (23.8)		
Grade 1	27 (51.9)	86 (55.8)	19 (45.2)		
Grade 2	19 (36.5)	32 (20.8)	13 (31.0)		
Grade 3	3 (5.8)	1 (0.6)	0		
ACR TI-RADS				0.019*	<0.001*
TR4	25 (48.1)	1 (0.6)	31 (73.8)		
TR5	27 (51.9)	153 (99.4)	11 (26.2)		

*, P<0.05 was considered statistically significant. US, ultrasound; PTL, primary thyroid lymphoma; PTC, papillary thyroid carcinoma; NHT, nodular Hashimoto's thyroiditis; ACR, American College of Radiology; TI-RADS, Thyroid Imaging Reporting and Data System.

to the different size distributions of NHT, PTC, and PTL nodules. Unexpectedly, we found that all relative parameters of qualitative and quantitative CEUS had no significant difference in nodules of different sizes (Tables S1-S3).

Comparison of diagnostic performances

The risk factors for malignant thyroid nodules combined

with HT are shown in Figures S1,S2. The diagnostic results of US, CEUS, and TIC in differentiating thyroid malignancies in patients with HT are shown in Table 5 and Figure 3. TIC parameters showed more effective in differentiating NHT and PTL (sensitivity of 84.62%, specificity of 97.62%, AUC of 0.947), but not as effective as conventional US in differentiating NHT and PTC (sensitivity of 90.91%, specificity of 73.81%, and AUC of

Table 3 Comparison of CEUS qualitative parameters in thyroid nodules combined with Hashimoto's thyroiditis

CEUS parameters	PTL (n=52), No. (%)	PTC (n=154), No. (%)	NHT (n=42), No. (%)	P	
				PLT vs. NHT	PTC vs. NHT
Enhancement direction				<0.001*	<0.001*
Scattered	0	11 (7.1)	23 (54.8)		
Centripetal/fugal	52 (100.0)	143 (92.9)	19 (45.2)		
Enhancement pattern				<0.001*	<0.001*
Homogeneous	1 (1.9)	1 (0.6)	21 (50.0)		
Heterogeneous	51 (98.1)	153 (99.4)	21 (50.0)		
Enhancement intensity				<0.001*	<0.001*
Hypo-enhancement	49 (94.2)	143 (92.9)	23 (54.8)		
Iso-enhancement	3 (5.8)	2 (1.3)	19 (45.2)		
Hyper-enhancement	0	9 (5.8)	0		

*, P<0.05 was considered statistically significant. CEUS, contrast-enhanced ultrasound; PTL, primary thyroid lymphoma; PTC, papillary thyroid carcinoma; NHT, nodular Hashimoto's thyroiditis.

Table 4 Comparison of TIC qualitative parameters in thyroid nodules combined with Hashimoto's thyroiditis

TIC parameters	PTL (n=52)	PTC (n=154)	NHT (n=42)	P	
				PTL vs. NHT	PTC vs. NHT
PI (dB)					
Lesion	13.07±3.24	12.55±3.05	15.37±2.62	<0.001*	<0.001*
Parenchyma	15.79±2.47	14.97±2.18	15.96±2.14	0.747	<0.001*
Ratio	0.84±0.13	0.92±0.13	0.97±0.10	<0.001*	0.710
RT (s)					
Lesion	19.78±3.19	19.67±3.93	20.66±3.94	0.357	0.029*
Parenchyma	21.65±4.20	19.59±3.90	21.01±4.19	0.139	0.282
Ratio	0.89±0.10	0.96±0.09	0.97±0.11	<0.001*	0.057
TTP (s)					
Lesion	30.31±5.82	29.89±6.40	32.55±6.10	0.049*	0.044*
Parenchyma	32.32±6.80	30.77±5.70	31.74±7.36	0.342	0.334
Ratio	0.90±0.10	0.97±0.10	1.00±0.09	<0.001*	0.175
TPH (s)					
Lesion	136.67±12.75	121.04±6.78	119.74±6.76	<0.001*	0.640
Parenchyma	128.50±18.18	120.20±6.53	119.47±6.61	<0.001*	0.807
Ratio	1.01±0.11	1.01±0.02	1.00±0.03	0.052	0.108
MTT (s)					
Lesion	24.03±5.42	23.47±4.44	24.69±5.69	0.858	0.843
Parenchyma	25.12±5.21	24.09±3.97	23.63±6.69	0.551	0.876
Ratio	0.96±0.13	0.99±0.14	0.98±0.09	0.403	0.446
AUC (dB sec)					
Lesion	1,683.31±289.65	1,541.61±235.50	1,886.24±302.87	<0.001*	<0.001*
Parenchyma	2,022.87±310.77	1,674.65±231.68	1,951.04±297.61	0.091	<0.001*
Ratio	0.85±0.13	0.93±0.14	0.98±0.11	<0.001*	0.006*

Data were presented as median ± interquartile range. *, P<0.05 was considered statistically significant. TIC, time-intensity curve; PTL, primary thyroid lymphoma; PTC, papillary thyroid carcinoma; NHT, nodular Hashimoto's thyroiditis; PI, peak intensity; RT, rise time; TTP, time to peak; TPH, time from peak to one-half; MTT, mean transit time; AUC, area under the curve.

Table 5 Comparison of diagnostic performances in differentiation thyroid nodules combined with Hashimoto's thyroiditis.

Variables	AUC (95% CI)	Sensitivity (%)	Specificity (%)	Youden index
PTL vs. NHT				
US	0.808 (0.721–0.894)	55.77	90.48	0.463
CEUS	0.774 (0.671–0.876)	100.00	54.76	0.548
TIC	0.947 (0.903–0.991)	84.62	97.62	0.822
US + CEUS	0.866 (0.795–0.938)	100.00	54.76	0.548
US + TIC	0.940 (0.892–0.988)	86.54	92.86	0.794
CEUS + TIC	0.965 (0.935–0.995)	88.46	92.86	0.813
US + CEUS + TIC	0.972 (0.945–0.998)	92.31	90.48	0.827
PTC vs. NHT				
US	0.954 (0.915–0.994)	87.66	92.86	0.805
CEUS	0.747 (0.646–0.847)	99.35	50.00	0.404
TIC	0.838 (0.759–0.917)	90.91	73.81	0.647
US + CEUS	0.960 (0.921–1.000)	92.86	90.48	0.833
US + TIC	0.968 (0.935–1.000)	94.81	92.86	0.877
CEUS + TIC	0.914 (0.858–0.970)	88.96	80.95	0.699
US + CEUS + TIC	0.975 (0.952–0.999)	90.91	95.24	0.862

US, ultrasound; CEUS, contrast-enhanced ultrasound; TIC, time-intensity curve; PTL, primary thyroid lymphoma; PTC, papillary thyroid carcinoma; NHT, nodular Hashimoto's thyroiditis; AUC, area under the receiver operating characteristic curve; CI, confidence interval.

0.838). Compared with using US, CEUS, or TIC alone, the combination of US, CEUS, and TIC had the best sensitivity, specificity, and AUC. The sensitivity, specificity, AUC, and Youden index in diagnosis between PTL and NHT were 92.31%, 90.48%, 0.972, and 0.827, respectively. The sensitivity, specificity, AUC, and Youden index in distinguishing between PTC and NHT were 90.91%, 95.24%, 0.975, and 0.862, respectively.

Discussion

This study mainly explored the diagnostic value of quantitative CEUS using TIC analysis in the differentiation of thyroid nodules coexistent with diffuse HT, and compared its diagnostic accuracy with that of qualitative US and CEUS.

Previous research discovered that grey-scale US characteristics of PTC commonly include microcalcifications, a taller than wide shape, and extrathyroidal extension (13). However, few studies have investigated whether the above features also apply to

malignant nodules in the presence of HT in the thyroid parenchymal background, and the HT background often interferes with the discrimination of malignant nodules. Our research compared the US characteristics of NHT to those of PTC. The results showed that PTC is more likely to have a taller than wide shape, extrathyroidal extension, micro-calcification, and posterior echo attenuation US characteristics when accompanied by HT background, compared to NHT. However, some studies have considered that conventional US characteristics, such as margin and calcification, were difficult to identify in the heterogeneous thyroid gland coexisting with HT (29). PTL has a few common features with other malignant nodules on conventional US, such as micro-calcification or taller than wide shape (10). Furthermore, grey-scale US and color Doppler US images are inadequate in distinguishing between NHT and PTL. This difficulty arises because PTL exhibits more overlapping signs with HT on US images, whereas conventional US characteristics may lack the sensitivity to detect subtle changes (14,30). Our study demonstrated that conventional US features only

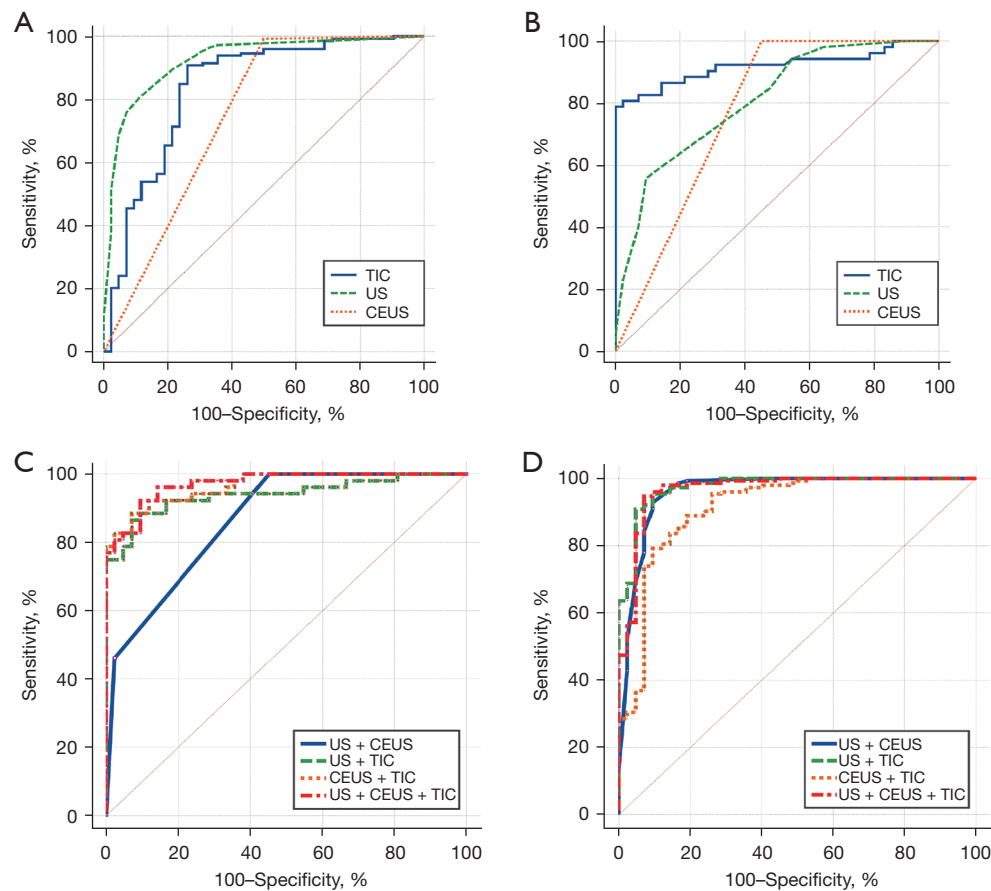


Figure 3 Comparison of diagnostic performances between conventional US, CEUS, TIC, and their combination. (A,C) The ROC curves based on differentiation PTC and NHT. (B,D) The ROC curves based on differentiation PTL and NHT. TIC, time-intensity curve; US, ultrasound; CEUS, contrast-enhanced ultrasound; ROC, receiver operating characteristic; PTC, papillary thyroid carcinoma; NHT, nodular Hashimoto's thyroiditis; PTL, primary thyroid lymphoma.

with posterior acoustic enhancement and extrathyroidal extension were likely to be thyroid lymphoma, which is consistent with previous findings (31). In conclusion, intranodular vascularity itself, as well as a combination of vascularity and suspicious gray-scale US features, did not perform as well as gray-scale US features in differentiating benign and malignant thyroid nodules. The ACR TI-RADS classification of our selected nodules focused on TR4 as well as TR5, and the TI-RADS grading was statistically different between NHT and malignant lesions (PTC and PTL). However, we agree that there is a significant overlap between benign and malignant nodules in ACR TI-RADS classifications 4 and 5, especially for nodules coexisting with HT (29). Furthermore, we chose nodules with definitive pathological findings after biopsy or surgery in our study, and the US features of the selected lesions were more likely

to be solid and hypoechoic, which are considered suspicious for malignancy in ACR TI-RADS. Another statistically significant finding in our study was the centripetal, heterogeneous, and hypo enhancement pattern for the detection of malignant lesions (PTC and PTL) ($P < 0.001$). This finding is in concordance with other studies that have indicated that heterogeneous hypo-enhancement is the most precise predictor of malignancy on CEUS with improved diagnostic performance (20,29,32,33); however, our study did not show high sensitivity, specificity, and accuracy using CEUS features. In fact, these three CEUS features were also identified in roughly 50% of the NHT lesions in our study. The presentation may be due to the fact that the heterogeneous and highly vascularized nature of the thyroid tissue can affect the contrast enhancement pattern between the lesion and surrounding tissue (30). Some researchers

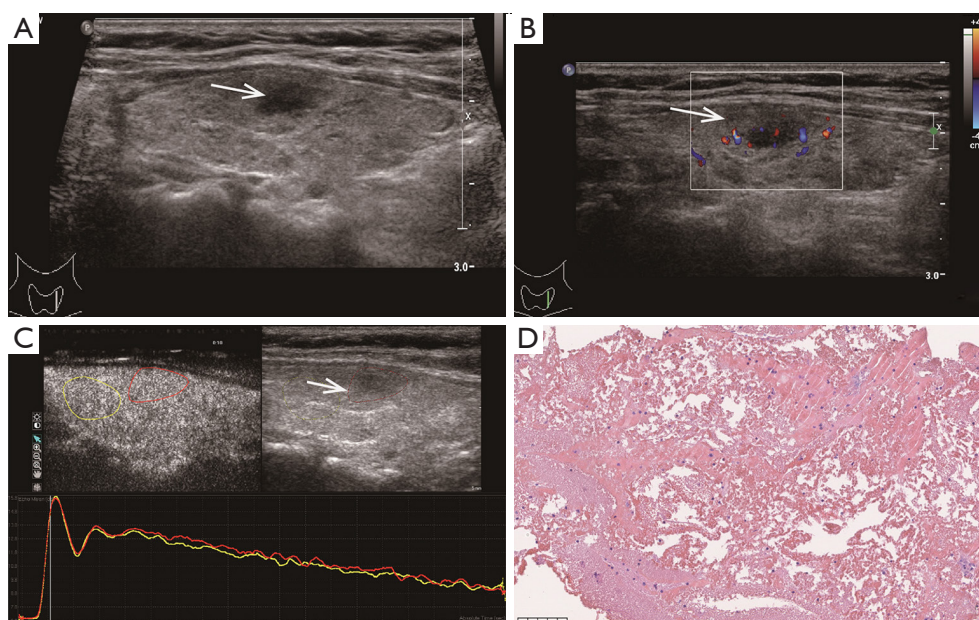


Figure 4 A 45-year-old female was found to have a 13 mm × 9 mm × 12 mm solid nodule in a background of heterogeneous parenchyma. (A) Grey-scale ultrasound showed this lesion (arrow) in the left lobe of thyroid had irregular margin and hypoechoic. (B) Color Doppler ultrasound showed this lesion (arrow) in the left lobe of thyroid had Adler grade 3. (C) The TIC showed this lesion (arrow) and thyroid parenchyma both had homogeneous iso-enhancement after injection of contrast agent. Red circles represented ROI that was placed on the thyroid nodules. Yellow circles were drawn in the adjacent thyroid parenchyma as an internal reference. (D) The pathological diagnosis after biopsy was a nodular Hashimoto's thyroiditis (HE staining, ×40). TIC, time-intensity curve; ROI, region of interest; HE, hematoxylin and eosin.

have suggested that CEUS in the characterization of thyroid nodules has a relationship with the size of the nodules (24). However, in our study, we concluded that CEUS features showed no significant differences between groups of different nodule sizes. We believe that this may be because we excluded tiny nodules (<10 mm) that were not suitable for CEUS imaging observation at the stage of patient inclusion. In addition, larger data should be evaluated and the role of TIC in CEUS patterns should be further assessed. We believe that it would be more reliable to continue to expand the data in question to investigate whether nodule size has an effect on CEUS parameters or not, and that a larger amount of data would yield more reliable results.

TIC analysis revealed that thyroid malignancies (PTC and PTL) showed significantly faster perfusion and lower intensity than did NHT, which was consistent with the previous studies (18,34). This might be explained by that thyroid benign nodules showed profuse, regular, and intra-nodular vascularity (18). In contrast, low-efficiency vascularity was often seen in thyroid malignant

nodules, possibly due to calcifications, focal necrosis, and internal microthrombi (23). PTL tended to exhibit a later clearance than did NHT lesions, which might be somewhat contradictory to the prior literature involving TIC analysis reporting that malignant nodules are apt to go early perfusion and early clearance (23). The intra-nodule perfusion of PTL showed obvious slower perfusion and lower PI compared to the background parenchyma. Therefore, we performed pathological analysis to identify the pathological background explaining the paradox between our observation and others (*Figures 4-6*). We primarily analyzed the different ultrasonographic manifestations of the lesion from the pathological images and our samples were larger than those in previous studies. In pathological analysis, PTL usually shows increased fibrotic structures and microvascular changes after lymphocytic infiltration (10), and larger thyroid malignant nodules tend to show focal necrosis (22). PTL in our study appeared to have a later clearance, which may be related to alterations in the number, arrangement, and role of blood vessels (35), or to a particularly large size compared to that of other thyroid

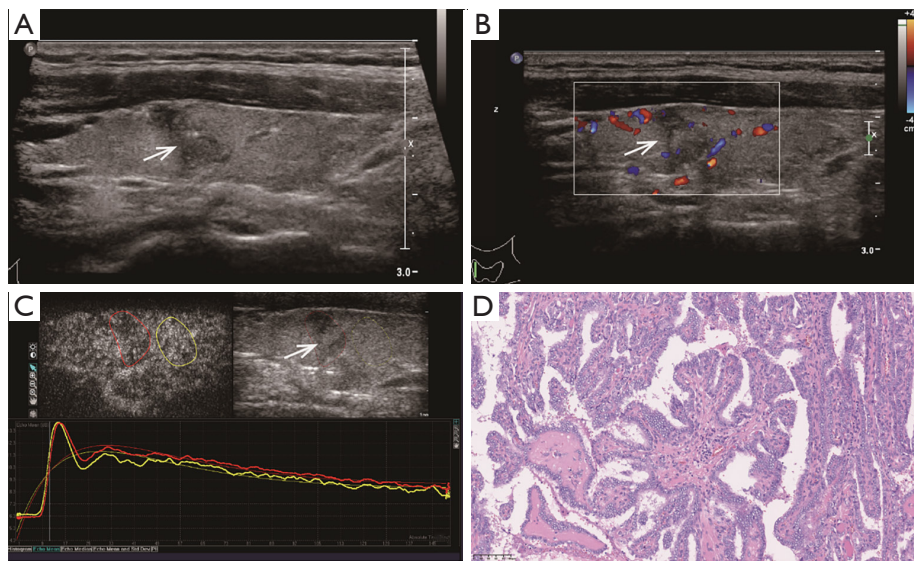


Figure 5 A 23-year-old male was found to have a 12 mm × 8 mm × 6 mm solid nodule in a background of heterogeneous parenchyma. (A) Grey-scale ultrasound showed this lesion (arrow) in the right lobe of thyroid had hypoechoic, taller than wide shape, microcalcification, and extra-thyroidal extension margin. (B) Color Doppler ultrasound showed this lesion (arrow) in the right lobe of thyroid had Adler grade 2. (C) The TIC showed this lesion (arrow) had lower heterogeneous hypo-enhancement than the thyroid parenchyma after injection of contrast agent. Red circles represent the ROI that was placed on the thyroid nodules. Yellow circles were drawn in the adjacent thyroid parenchyma as an internal reference. (D) The pathological diagnosis after surgery was a papillary thyroid carcinoma (HE staining, ×40). TIC, time-intensity curve; ROI, region of interest; HE, hematoxylin and eosin.

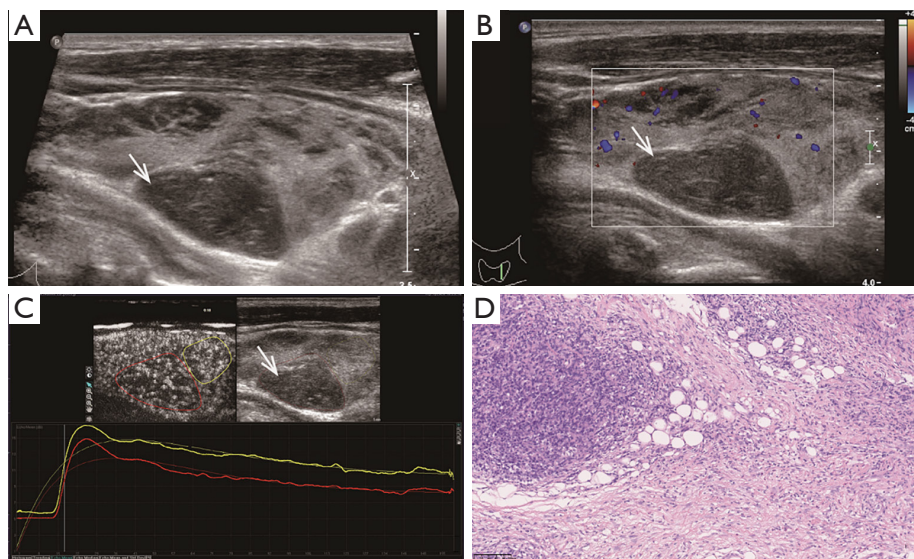


Figure 6 A 66-year-old male was found to have a 24 mm × 14 mm × 14 mm solid nodule in a background of heterogeneous parenchyma. (A) Grey-scale ultrasound showed this lesion (arrow) in the left lobe of thyroid had wider than tall shape and markedly hypoechoic. (B) Color Doppler ultrasound showed this lesion (arrow) in the left lobe of thyroid had Adler grade 0. (C) The TIC showed this lesion (arrow) had much lower heterogeneous hypo-enhancement than the thyroid parenchyma after injection of contrast agent. Red circles represent the ROI that was placed on the thyroid nodules. Yellow circles were drawn in the adjacent thyroid parenchyma as an internal reference. (D) The pathological diagnosis after biopsy was a primary thyroid lymphoma (HE staining, ×40). TIC, time-intensity curve; ROI, region of interest; HE, hematoxylin and eosin.

malignant nodules. Thus, the TIC parameters may provide quantitative complementary information to US and CEUS results regarding the microvascular characteristics of NHT and malignant nodules (PTC and PTL).

Our results indicated that CEUS showed relatively poorer performance when conventional US, CEUS, and TIC were used respectively for nodule classification. Wang *et al.* also argued that CEUS was inadequate to differentiate benign from malignant ACR TIRADS 4 and 5 category nodules coexisting with HT (29). In our study, combining the above three US modalities for the differential diagnosis of NHT from malignant nodules (PTC and PTL) resulted in an at least 3% improvement in diagnostic performance (AUC). Adding qualitative and quantitative CEUS features to the TI-RADS classification, which currently relies only on grey-scale mode, would be a meaningful improvement. Ruan *et al.* constructed the CEUS TI-RADS by adding CEUS to widely accepted nonenhanced US features based on ACR TI-RADS (36). This would help to standardize the process of evaluating CEUS for thyroid nodules. However, overlapping data between CEUS qualitative and quantitative evaluation parameters and criteria of benign and malignant nodules indicate a limitation in the interpretation of tumor microvasculature. The EFSUMB guidelines suggested that no single indicator is sufficiently sensitive or specific (19). Thus, to improve the diagnostic performance in thyroid nodules with HT, the results should be interpreted in conjunction with clinical data, conventional US, and other imaging findings.

There are several limitations in our study. First, we did not include more nodules of different sizes and normal backgrounds as controls for comparison. Due to sample selection bias, we had a limited range of pathological types (only including NHT, PTC, and PTL). We failed to reflect all of the CEUS characteristics associated with thyroid nodules compared with some studies involving CEUS (36,37), which may have affected the assessment of the diagnostic performance of qualitative CEUS. However, we designed this study as a preliminary study investigating the feasibility of quantitative CEUS analysis for the distinction of thyroid nodules with HT. Second, a lack of reproducibility is one of the major obstacles to quantitative assessment in imaging studies including CEUS. Our study used a single type of contrast agent and US machine; generalization of our results to other contrast agents and machine requires caution. We used different doses depending on the size of the nodule, generally 1 mL for the US scan of the patient and 2 mL for patients with larger

nodules (≥ 50 mm). There is no evidence that this affected the results, but we supposed it could be a potential bias factor. Our study only had one reader to draw the ROIs and this may have introduced some subjective bias regarding selecting locations and determining the size of the ROIs. These limitations affected the outcome of enhancement evaluation and produced a certain deviation. Thus, some studies have suggested that quantitative CEUS analysis could be of little importance (37).

In conclusion, a quantitative analysis of nodular microvascularization with CEUS can provide useful additional information to differentiate thyroid nodules under HT, compared with unstable visual diagnostic US criteria of nodule morphology and vascularity. This method may have the potential to reduce unnecessary biopsies.

Acknowledgments

Funding: This work was supported by a grant from the Department of Science and Technology of Sichuan Province (No. 2018RZ0138).

Footnote

Reporting Checklist: The authors have completed the STARD reporting checklist. Available at <https://qims.amegroups.com/article/view/10.21037/qims-23-601/rc>

Conflicts of Interest: All authors have completed the ICMJE uniform disclosure form (available at <https://qims.amegroups.com/article/view/10.21037/qims-23-601/coif>). The authors have no conflicts of interest to declare.

Ethical Statement: The authors are accountable for all aspects of the work in ensuring that questions related to the accuracy or integrity of any part of the work are appropriately investigated and resolved. The study was conducted in accordance with the Declaration of Helsinki (as revised in 2013). The study was approved by the Ethics Committee on Biomedical Research of West China Hospital, Sichuan University (No. 20230927). The committee waived the requirement for individual consent for this retrospective analysis.

Open Access Statement: This is an Open Access article distributed in accordance with the Creative Commons Attribution-NonCommercial-NoDerivs 4.0 International License (CC BY-NC-ND 4.0), which permits the non-

commercial replication and distribution of the article with the strict proviso that no changes or edits are made and the original work is properly cited (including links to both the formal publication through the relevant DOI and the license). See: <https://creativecommons.org/licenses/by-nc-nd/4.0/>.

References

- Miranda-Filho A, Lortet-Tieulent J, Bray F, Cao B, Franceschi S, Vaccarella S, Dal Maso L. Thyroid cancer incidence trends by histology in 25 countries: a population-based study. *Lancet Diabetes Endocrinol* 2021;9:225-34.
- Pizzato M, Li M, Vignat J, Laversanne M, Singh D, La Vecchia C, Vaccarella S. The epidemiological landscape of thyroid cancer worldwide: GLOBOCAN estimates for incidence and mortality rates in 2020. *Lancet Diabetes Endocrinol* 2022;10:264-72.
- Ferrari SM, Fallahi P, Elia G, Ragusa F, Ruffilli I, Paparo SR, Antonelli A. Thyroid autoimmune disorders and cancer. *Semin Cancer Biol* 2020;64:135-46.
- Antonelli A, Ferrari SM, Corrado A, Di Domenicantonio A, Fallahi P. Autoimmune thyroid disorders. *Autoimmun Rev* 2015;14:174-80.
- Ralli M, Angeletti D, Fiore M, D'Aguzzo V, Lambiase A, Artico M, de Vincentiis M, Greco A. Hashimoto's thyroiditis: An update on pathogenic mechanisms, diagnostic protocols, therapeutic strategies, and potential malignant transformation. *Autoimmun Rev* 2020;19:102649.
- Resende de Paiva C, Grønhoj C, Feldt-Rasmussen U, von Buchwald C. Association between Hashimoto's Thyroiditis and Thyroid Cancer in 64,628 Patients. *Front Oncol* 2017;7:53.
- Travaglini A, Pace M, Varricchio S, Insabato L, Giordano C, Picardi M, Pane F, Staibano S, Mascolo M. Hashimoto Thyroiditis in Primary Thyroid Non-Hodgkin Lymphoma. *Am J Clin Pathol* 2020;153:156-64.
- Azizi G, Keller JM, Lewis M, Piper K, Puett D, Rivenbark KM, Malchoff CD. Association of Hashimoto's thyroiditis with thyroid cancer. *Endocr Relat Cancer* 2014;21:845-52.
- Sharma A, Jasim S, Reading CC, Ristow KM, Villasboas Bisneto JC, Habermann TM, Fatourechi V, Stan M. Clinical Presentation and Diagnostic Challenges of Thyroid Lymphoma: A Cohort Study. *Thyroid* 2016;26:1061-7.
- Stein SA, Wartofsky L. Primary thyroid lymphoma: a clinical review. *J Clin Endocrinol Metab* 2013;98:3131-8.
- Xu S, Huang H, Qian J, Liu Y, Huang Y, Wang X, Liu S, Xu Z, Liu J. Prevalence of Hashimoto Thyroiditis in Adults With Papillary Thyroid Cancer and Its Association With Cancer Recurrence and Outcomes. *JAMA Netw Open* 2021;4:e2118526.
- Malhi HS, Grant EG. Ultrasound of Thyroid Nodules and the Thyroid Imaging Reporting and Data System. *Neuroimaging Clin N Am* 2021;31:285-300.
- Gul K, Dirikoc A, Kiyak G, Ersoy PE, Ugras NS, Ersoy R, Cakir B. The association between thyroid carcinoma and Hashimoto's thyroiditis: the ultrasonographic and histopathologic characteristics of malignant nodules. *Thyroid* 2010;20:873-8.
- Anderson L, Middleton WD, Teefey SA, Reading CC, Langer JE, Desser T, Szabunio MM, Hildebolt CF, Mandel SJ, Cronan JJ. Hashimoto thyroiditis: Part 1, sonographic analysis of the nodular form of Hashimoto thyroiditis. *AJR Am J Roentgenol* 2010;195:208-15.
- Park M, Park SH, Kim EK, Yoon JH, Moon HJ, Lee HS, Kwak JY. Heterogeneous echogenicity of the underlying thyroid parenchyma: how does this affect the analysis of a thyroid nodule? *BMC Cancer* 2013;13:550.
- Alexander LF, Patel NJ, Caserta MP, Robbin ML. Thyroid Ultrasound: Diffuse and Nodular Disease. *Radiol Clin North Am* 2020;58:1041-57.
- Radzina M, Ratniece M, Putrins DS, Saule L, Cantisani V. Performance of Contrast-Enhanced Ultrasound in Thyroid Nodules: Review of Current State and Future Perspectives. *Cancers (Basel)* 2021;13:5469.
- Nemec U, Nemec SF, Novotny C, Weber M, Czerny C, Krestan CR. Quantitative evaluation of contrast-enhanced ultrasound after intravenous administration of a microbubble contrast agent for differentiation of benign and malignant thyroid nodules: assessment of diagnostic accuracy. *Eur Radiol* 2012;22:1357-65.
- Haugen BR, Alexander EK, Bible KC, Doherty GM, Mandel SJ, Nikiforov YE, Pacini F, Randolph GW, Sawka AM, Schlumberger M, Schuff KG, Sherman SI, Sosa JA, Steward DL, Tuttle RM, Wartofsky L. 2015 American Thyroid Association Management Guidelines for Adult Patients with Thyroid Nodules and Differentiated Thyroid Cancer: The American Thyroid Association Guidelines Task Force on Thyroid Nodules and Differentiated Thyroid Cancer. *Thyroid* 2016;26:1-133.
- Sidhu PS, Cantisani V, Dietrich CF, Gilja OH, Saftoiu A, Bartels E, et al. The EFSUMB Guidelines and Recommendations for the Clinical Practice of Contrast-Enhanced Ultrasound (CEUS) in Non-Hepatic Applications: Update 2017 (Long Version). *Ultraschall*

- Med 2018;39:e2-e44.
21. Trimboli P, Castellana M, Virili C, Havre RF, Bini F, Marinozzi F, D'Ambrosio F, Giorgino F, Giovannella L, Prosch H, Grani G, Radzina M, Cantisani V. Performance of contrast-enhanced ultrasound (CEUS) in assessing thyroid nodules: a systematic review and meta-analysis using histological standard of reference. *Radiol Med* 2020;125:406-15.
 22. Zhang P, Liu H, Yang X, Pang L, Gu F, Yuan J, Ding L, Zhang J, Luo W. Comparison of contrast-enhanced ultrasound characteristics of inflammatory thyroid nodules and papillary thyroid carcinomas using a quantitative time-intensity curve: a propensity score matching analysis. *Quant Imaging Med Surg* 2022;12:5209-21.
 23. Zhou X, Zhou P, Hu Z, Tian SM, Zhao Y, Liu W, Jin Q. Diagnostic Efficiency of Quantitative Contrast-Enhanced Ultrasound Indicators for Discriminating Benign From Malignant Solid Thyroid Nodules. *J Ultrasound Med* 2018;37:425-37.
 24. Gu F, Han L, Yang X, Liu H, Li X, Guo K, Zhao Z, Zhou X, Luo W. Value of time-intensity curve analysis of contrast-enhanced ultrasound in the differential diagnosis of thyroid nodules. *Eur J Radiol* 2018;105:182-7.
 25. Adler DD, Carson PL, Rubin JM, Quinn-Reid D. Doppler ultrasound color flow imaging in the study of breast cancer: preliminary findings. *Ultrasound Med Biol* 1990;16:553-9.
 26. Willemink MJ, Koszek WA, Hardell C, Wu J, Fleischmann D, Harvey H, Folio LR, Summers RM, Rubin DL, Lungren MP. Preparing Medical Imaging Data for Machine Learning. *Radiology* 2020;295:4-15.
 27. Tessler FN, Middleton WD, Grant EG. Thyroid Imaging Reporting and Data System (TI-RADS): A User's Guide. *Radiology* 2018;287:29-36.
 28. EI-Naggar AK, Chan JKC, Grandis JR, Takata T, Slootweg PJ, editors. WHO classification of head and neck Tumours (4th edition). Lyon: International Agency for Research on Cancer IARC; 2017.
 29. Wang B, Ou X, Yang J, Zhang H, Cui XW, Dietrich CF, Yi AJ. Contrast-enhanced ultrasound and shear wave elastography in the diagnosis of ACR TI-RADS 4 and 5 category thyroid nodules coexisting with Hashimoto's thyroiditis. *Front Oncol* 2022;12:1022305.
 30. Anderson L, Middleton WD, Teefey SA, Reading CC, Langer JE, Desser T, Szabunio MM, Mandel SJ, Hildebolt CF, Cronan JJ. Hashimoto thyroiditis: Part 2, sonographic analysis of benign and malignant nodules in patients with diffuse Hashimoto thyroiditis. *AJR Am J Roentgenol* 2010;195:216-22.
 31. Zhang X, Wei B, Nong L, Zhang H, Gao Y, Ou J. The usefulness of serial ultrasound in thyroid mucosa-associated lymphoid tissue lymphoma. *Front Endocrinol (Lausanne)* 2022;13:1054584.
 32. Ma JJ, Ding H, Xu BH, Xu C, Song LJ, Huang BJ, Wang WP. Diagnostic performances of various gray-scale, color Doppler, and contrast-enhanced ultrasonography findings in predicting malignant thyroid nodules. *Thyroid* 2014;24:355-63.
 33. Zhan J, Ding H. Application of contrast-enhanced ultrasound for evaluation of thyroid nodules. *Ultrasonography* 2018;37:288-97.
 34. Brandenstein M, Wiesinger I, Künzel J, Hornung M, Stroszczyński C, Jung EM. Multiparametric Sonographic Imaging of Thyroid Lesions: Chances of B-Mode, Elastography and CEUS in Relation to Preoperative Histopathology. *Cancers (Basel)* 2022.
 35. Moon HJ, Kwak JY, Kim MJ, Son EJ, Kim EK. Can vascularity at power Doppler US help predict thyroid malignancy? *Radiology* 2010;255:260-9.
 36. Ruan J, Xu X, Cai Y, Zeng H, Luo M, Zhang W, Liu R, Lin P, Xu Y, Ye Q, Ou B, Luo B. A Practical CEUS Thyroid Reporting System for Thyroid Nodules. *Radiology* 2022;305:149-59.
 37. Petrasova H, Slaisova R, Rohan T, Sary K, Kyclova J, Pavlik T, Kovalcikova P, Kazda T, Valek V. Contrast-Enhanced Ultrasonography for Differential Diagnosis of Benign and Malignant Thyroid Lesions: Single-Institutional Prospective Study of Qualitative and Quantitative CEUS Characteristics. *Contrast Media Mol Imaging* 2022;2022:8229445.

Cite this article as: Yang W, Zhou J, Yue C, He Y, Lei J, Chen Y, Ma B. Clinical value of contrast-enhanced ultrasound quantitative analysis for differentiating thyroid lesions in Hashimoto's thyroiditis patients. *Quant Imaging Med Surg* 2024;14(1):944-957. doi: 10.21037/qims-23-601

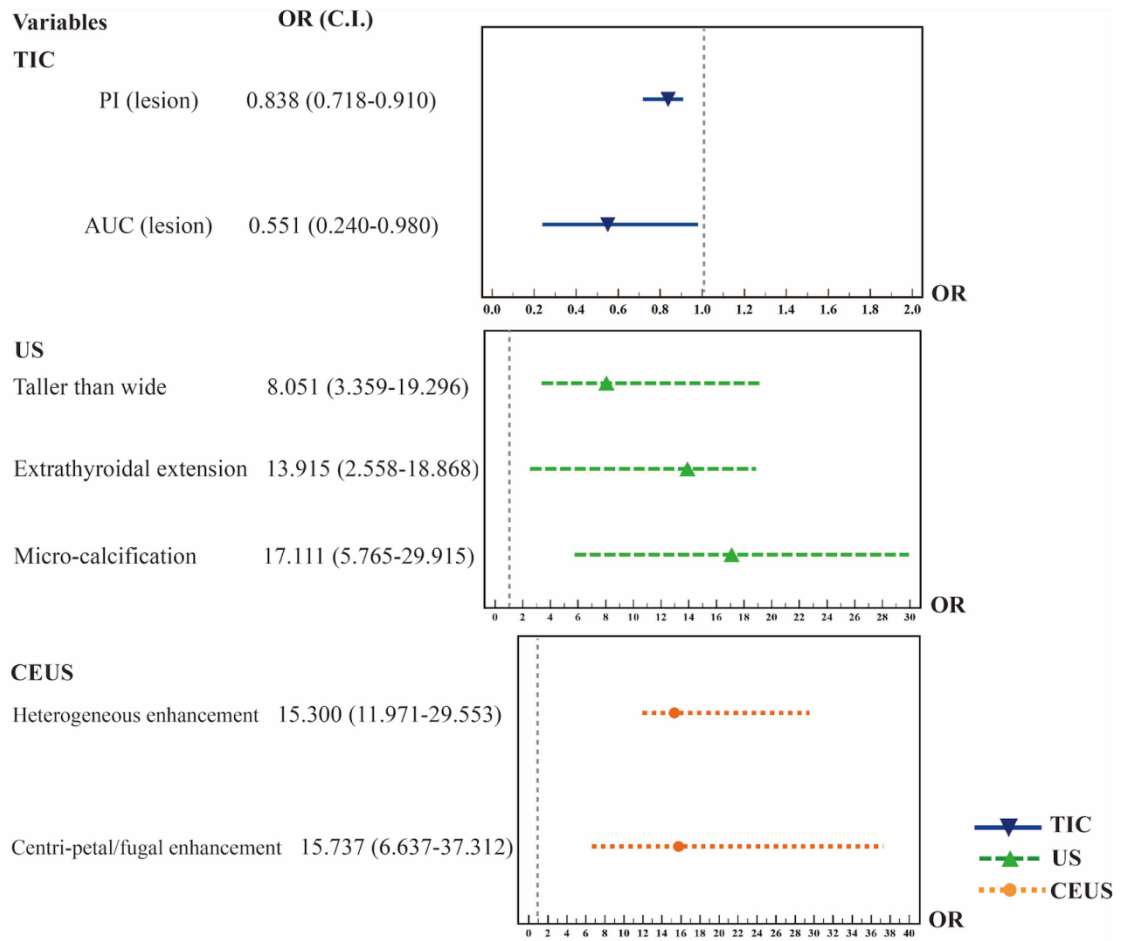


Figure S1 Forest plots of PTC and NHT based on the US, CEUS, and TIC features. Determined with multivariate analysis. PTC, papillary thyroid carcinoma; NHT, nodular Hashimoto's thyroiditis; US, ultrasound; CEUS, contrast-enhanced ultrasound; TIC, time-intensity curve; PI, peak intensity; AUC, area under the curve; OR, odds ratio; CI, confidence interval.

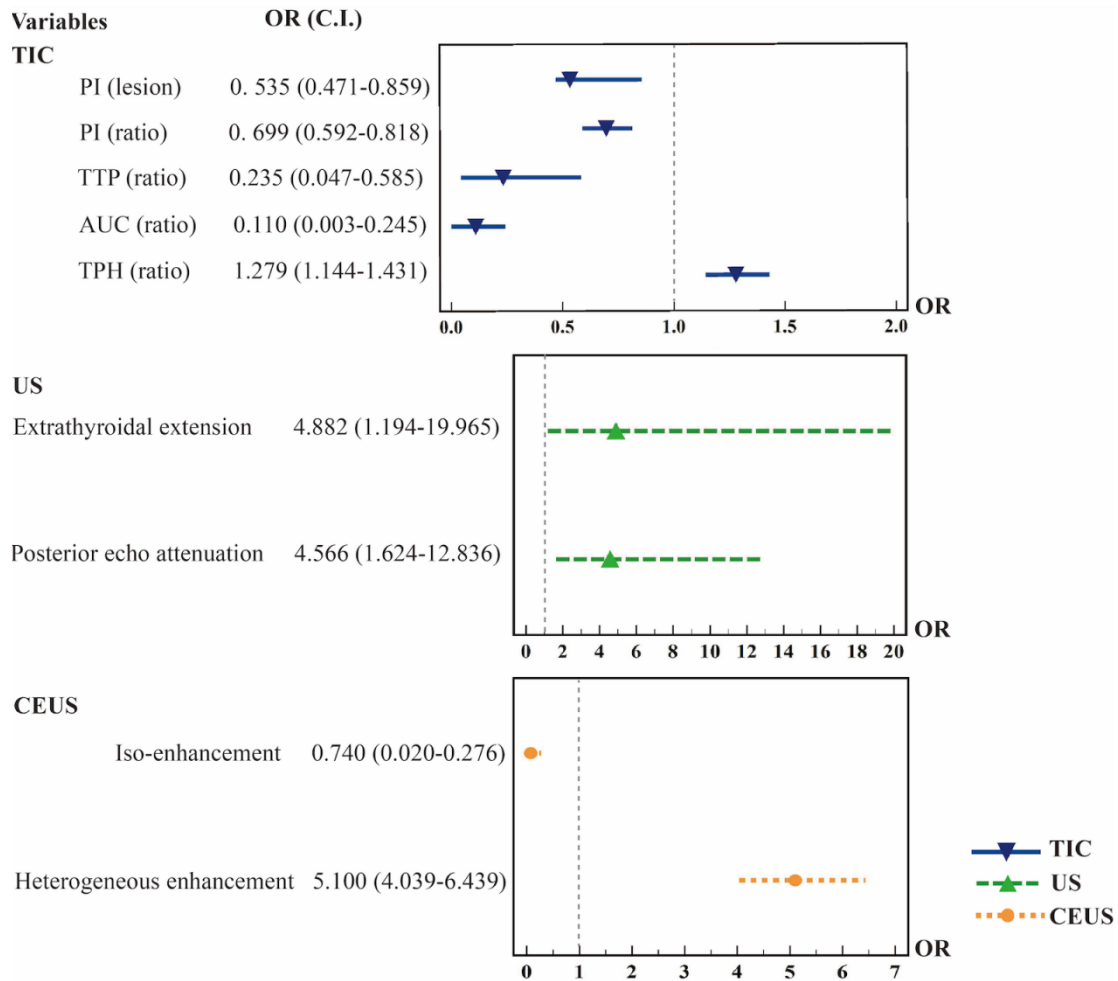


Figure S2 Forest plots of PTL and NHT based on the US, CEUS, and TIC features. Determined with multivariate analysis. PTL, primary thyroid lymphoma; NHT, nodular Hashimoto's thyroiditis; US, ultrasound; CEUS, contrast-enhanced ultrasound; TIC, time-intensity curve; PI, peak intensity; TTP, time to peak; AUC, area under the curve; TPH, time from peak to one-half; OR, odds ratio; CI, confidence interval.

Table S1 Comparison of qualitative and quantitative CEUS parameters PTC nodule size

Parameters	≥20 mm (n=40)	10–<20 mm (n=114)	P
Quantitative CEUS [†]			
PI (dB)			
Lesion	12.70±1.67	12.53±2.01	0.157
Parenchyma	13.72±1.55	13.69±1.92	0.204
Ratio	0.93±0.11	0.92±0.13	0.262
RT (s)			
Lesion	19.18±3.58	19.84±4.04	0.442
Parenchyma	20.63±4.09	20.42±3.88	0.815
Ratio	0.93±0.08	0.97±0.11	0.559
TTP (s)			
Lesion	30.31±5.82	29.89±6.40	0.605
Parenchyma	32.00±6.03	31.99±5.76	0.824
Ratio	0.95±0.08	0.99±0.17	0.492
TPH (s)			
Lesion	136.67±12.75	121.04±6.78	0.468
Parenchyma	119.26±8.18	118.95±7.08	0.335
Ratio	1.03±0.88	1.00±0.04	0.128
MTT (s)			
Lesion	23.81±4.33	25.19±6.16	0.435
Parenchyma	25.08±4.62	25.31±6.67	0.483
Ratio	0.96±0.11	1.01±0.20	0.536
AUC (dB sec)			
Lesion	1552.05±193.68	1537.41±249.19	0.077
Parenchyma	2022.87±310.77	1674.65±231.68	0.831
Ratio	0.94±0.12	0.93±0.15	0.901
Qualitative CEUS [‡]			
Enhancement direction			0.241
Scattered	5 (12.5)	6 (5.3)	
Centripetal/fugal	35 (87.5)	108 (94.7)	
Enhancement pattern			
Homogeneous	0	1 (0.9)	0.552
Heterogeneous	40 (100.0)	113 (99.1)	
Enhancement intensity			
Hypo-enhancement	36 (90.0)	107 (93.9)	0.309
Iso-enhancement	0	2 (1.8)	
Hyper-enhancement	4 (10.0)	5 (4.4)	

[†], data were presented as median ± interquartile range. [‡], data were numbers of patients, with percentages in parentheses. CEUS, contrast-enhanced ultrasound; PI, peak intensity; RT, rise time; TTP, time to peak; TPH, time from peak to one-half; MTT, mean transit time; AUC, area under the curve; PTC, papillary thyroid carcinoma.

Table S2 Comparison of qualitative and quantitative CEUS parameters PTL nodule size

Parameters	≥50 mm (n=38)	10–<50 mm (n=14)	P
Quantitative CEUS [†]			
PI (dB)			
Lesion	12.77±2.18	13.88±2.01	0.756
Parenchyma	15.74±2.35	13.34±1.53	0.211
Ratio	0.82±0.12	0.91±0.13	0.953
RT (s)			
Lesion	19.82±4.03	19.59±3.55	0.824
Parenchyma	22.38±5.22	21.75±3.02	0.301
Ratio	0.89±0.10	0.90±0.10	0.473
TTP (s)			
Lesion	30.28±6.22	30.26±4.51	0.678
Parenchyma	34.49±7.92	32.71±4.38	0.242
Ratio	0.88±0.10	0.92±0.07	0.119
TPH (s)			
Lesion	143.74±16.23	129.32±9.04	0.107
Parenchyma	129.50±16.21	126.86±8.23	0.335
Ratio	1.12±0.16	1.02±0.02	0.087
MTT (s)			
Lesion	24.62±5.00	23.97±3.32	0.487
Parenchyma	26.26±8.35	25.39±3.11	0.362
Ratio	0.96±0.15	0.95±0.07	0.536
AUC (dB s)			
Lesion	1676.76±310.25	1717.21±226.45	0.317
Parenchyma	2022.87±310.77	1674.65±231.68	0.214
Ratio	0.82±0.13	0.91±0.12	0.651
Qualitative CEUS [‡]			
Enhancement direction			0.110
Scattered	1 (2.6)	2 (14.3)	
Centripetal/fugal	37 (97.4)	12 (85.7)	
Enhancement pattern			
Homogeneous	0	1 (7.1)	0.096
Heterogeneous	38 (100.0)	13 (92.9)	
Enhancement intensity			
Hypo-enhancement	37 (97.4)	12 (85.7)	0.110
Iso-enhancement	1 (2.6)	2 (14.3)	
Hyper-enhancement	0	0	

[†], data were presented as median ± interquartile range. [‡], data were numbers of patients, with percentages in parentheses. CEUS, contrast-enhanced ultrasound; PI, peak intensity; RT, rise time; TTP, time to peak; TPH, time from peak to one-half; MTT, mean transit time; AUC, area under the curve; PTL, primary thyroid lymphoma.

Table S3 Comparison of qualitative and quantitative CEUS parameters NHT nodule size

Parameters	≥20 mm (n=15)	10–<20 mm (n=27)	P
Quantitative CEUS [†]			
PI (dB)	12.77±2.18	13.88±2.01	0.064
Lesion	16.29±1.53	15.16±2.11	0.403
Parenchyma	0.94±0.10	0.97±0.10	0.784
Ratio			
RT (s)	21.19±4.20	20.36±3.83	0.824
Lesion	21.79±4.49	20.57±3.73	0.384
Parenchyma	0.98±0.10	0.99±0.07	0.177
Ratio			
TTP (s)	32.90±5.89	32.36±6.31	0.099
Lesion	33.76±7.25	32.28±5.64	0.458
Parenchyma	0.98±0.10	0.99±0.07	0.646
Ratio			
TPH (s)	119.16±5.93	120.06±7.27	0.107
Lesion	118.28±7.22	120.13±6.28	0.473
Parenchyma	1.00±0.03	1.01±0.02	0.412
Ratio			
MTT (s)	24.52±3.75	24.78±3.59	0.360
Lesion	24.61±4.01	25.65±5.76	0.362
Parenchyma	0.98±0.09	0.97±0.10	0.829
Ratio			
AUC (dB sec)	1901.54±182.36	1877.73±355.72	0.036*
Lesion	2031.59±239.71	1870.04±269.22	0.689
Parenchyma	0.95±0.12	0.97±0.11	0.664
Ratio			
Qualitative CEUS [‡]			
Enhancement direction			0.152
Scattered	6 (40.0)	17 (63.0)	
Centripetal/fugal	9 (60.0)	10 (37.0)	
Enhancement pattern			0.334
Homogeneous	6 (40.0)	15 (55.6)	
Heterogeneous	9 (60.0)	12 (44.4)	
Enhancement intensity			0.611
Hypo-enhancement	6 (40.0)	13 (48.1)	
Iso-enhancement	9 (60.0)	14 (51.9)	
Hyper-enhancement	0	0	

*, P<0.05 was considered statistically significant. [†], data were presented as median ± interquartile range. [‡], data were numbers of patients, with percentages in parentheses. CEUS, contrast-enhanced ultrasound; PI, peak intensity; RT, rise time; TTP, time to peak; TPH, time from peak to one-half; MTT, mean transit time; AUC, area under the curve; NHT, nodular Hashimoto's thyroiditis